AD-A133 508 TWO-STAGE FEL (FREE ELECTRON LASER) PROGRAM(U) KMS 1/1
FUSION INC ANN ARBOR MI S B SEGALL ET AL. 25 AUG 83
KMSF-U1359 N00014-80-C-0614

UNCLASSIFIED F/G 20/5 NL

END

FILMED

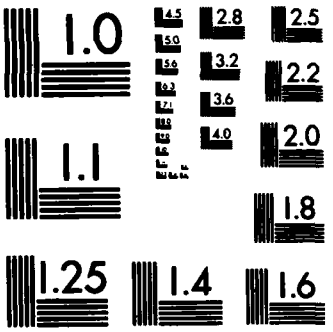

MICROCOPY RESOLUTION TEST CHART
NATIONAL BUREAU OF STANDARDS-1963-A

KMSF-01359

kms fusion inc.

THE KMS FUSION, INC., TWO-STAGE FEL PROGRAM

S. B. Segall, H. Takeda and S. Von Laven

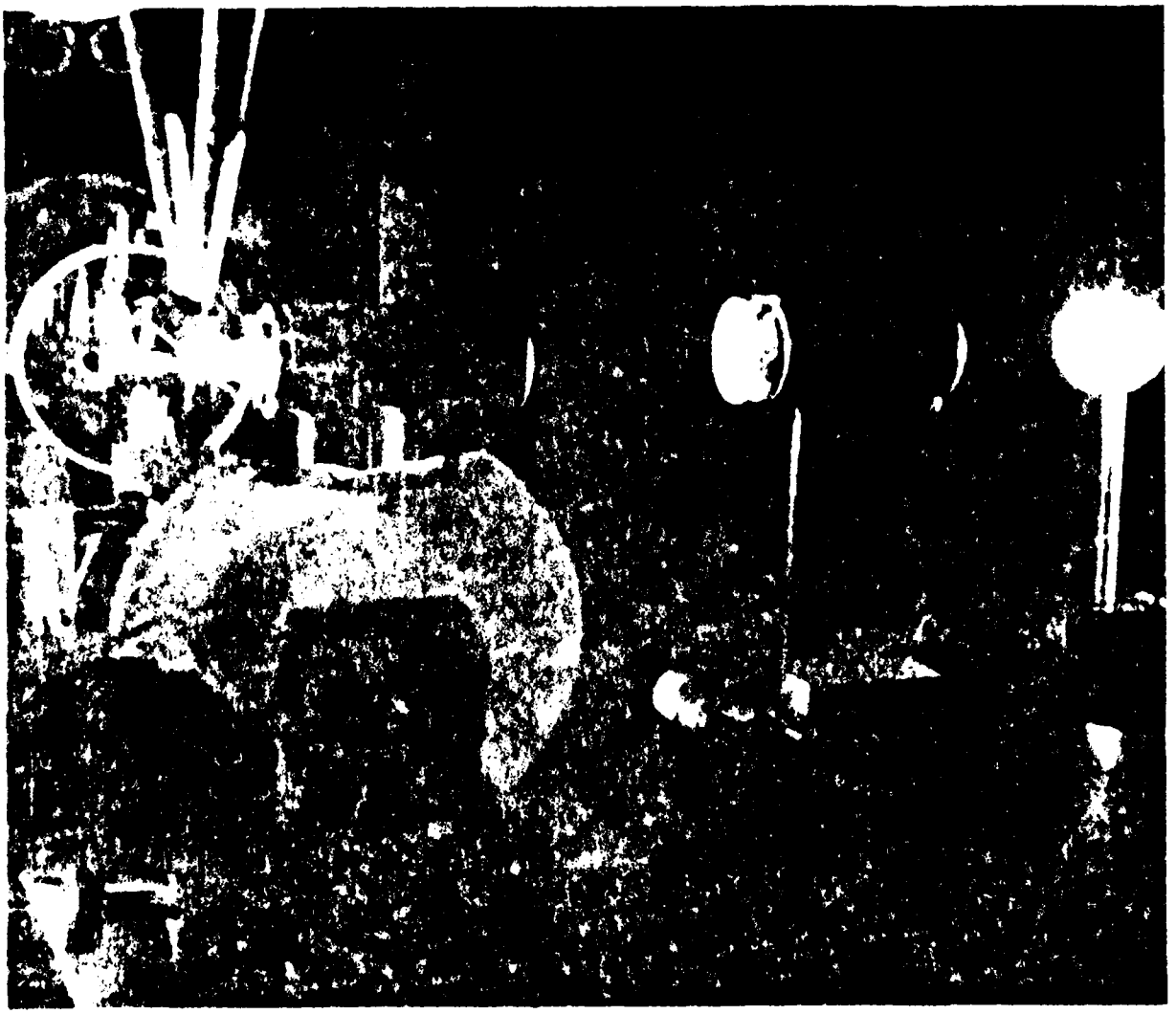

Submitted to: SPIE (International Society for Optical Engineering) Bellingham, Washington

SECURITY CLASSIFICATION OF THIS PAGE (When Data Entered)

REPORT DOCUMENTATION PAGE		READ INSTRUCTIONS BEFORE COMPLETING FORM
1. REPORT NUMBER KMSF-U1359	2. GOVT ACCESSION NO. AD-A133508	3. RECIPIENT'S CATALOG NUMBER
4. TITLE (and Subtitle) The KMS Fusion Inc., two-stage free electron laser program		5. TYPE OF REPORT & PERIOD COVERED Technical Report 6. PERFORMING ORG. REPORT NUMBER
7. AUTHOR(s) S. B. Segall, H. Takeda, S. Von Laven, P. Diament, and J. F. Ward		8. CONTRACT OR GRANT NUMBER(s) N00014-80-C-0614
9. PERFORMING ORGANIZATION NAME AND ADDRESS KMS Fusion, Inc. 3621 South State Road, P.O. Box 1567 Ann Arbor, MI 48106		10. PROGRAM ELEMENT, PROJECT, TASK AREA & WORK UNIT NUMBERS
11. CONTROLLING OFFICE NAME AND ADDRESS Defense Contract Administration Services Management Area, Detroit McNamara Federal Bldg., 477 Michigan Avenue Detroit, MI 48226		12. REPORT DATE August 25, 1983 13. NUMBER OF PAGES 11
14. MONITORING AGENCY NAME & ADDRESS (if different from Controlling Office) Office of Naval Research 1030 Green Street Pasadena, CA 91106		15. SECURITY CLASS. (of this report) Unclassified 15a. DECLASSIFICATION/DOWNGRADING SCHEDULE

16. DISTRIBUTION STATEMENT (of this Report)

Unlimited

17. DISTRIBUTION STATEMENT (of the abstract entered in Block 20, if different from Report)

18. SUPPLEMENTARY NOTES

To be published in the proceedings of the FEL Workshop held at Eastsound, WA, June, 1983

19. KEY WORDS (Continue on reverse side if necessary and identify by block number)

Free electron laser, quasioptical cavity, waveguide laser, wiggler magnet, helical wiggler, two-stage FEL, phase space displacement

20. ABSTRACT (Continue on reverse side if necessary and identify by block number)

A review of the two-stage free electron laser (FEL) research program at KMS Fusion, Inc. is presented. The work includes cavity and wiggler magnet design, a study of methods for minimizing electron energy spread at high first stage intensity, and calculations of second-stage gain. A quasioptical cavity is proposed to contain the first-stage long-wavelength radiation while permitting transmission of second-stage short-wavelength radiation. A permanent magnet helical wiggler will be used to produce the long-wavelength radiation. At

DD FORM 1 JAN 73 1473 EDITION OF 1 NOV 65 IS OBSOLETE

SECURITY CLASSIFICATION OF THIS PAGE (When Data Entered)

high first-stage intensities ($\sim 10^8$ W/cm^2) the energy spread produced in the wiggler will be $\geq 10\%$. For the experiment being proposed the beam line and electron collector must be modified to accept this spread. Companion papers in this volume give additional details of the cavity design and minimization of energy spread.

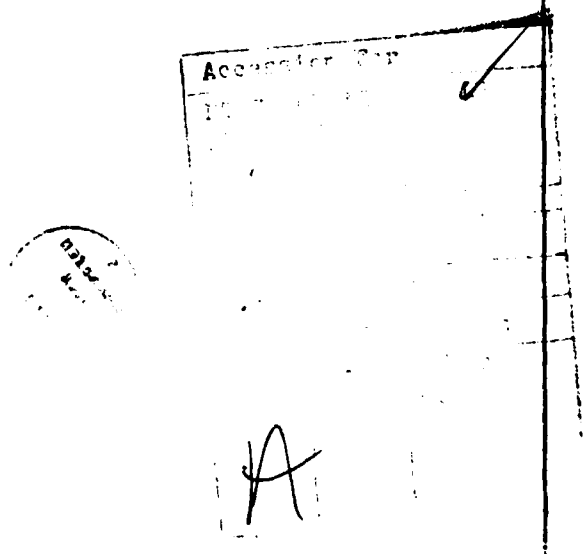

The KMS Fusion, Inc. two-stage free electron laser program

S. B. Segall, H. Takeda and S. Von Laven
KMS Fusion, Inc., Ann Arbor, MI 48106

P. Diament, Columbia University, New York, NY 10027
J. F. Ward, University of Michigan, Ann Arbor, MI 48109

Abstract

A review of the two-stage free electron laser (FEL) research program at KMS Fusion, Inc. is presented. The work includes cavity and wiggler magnet design, a study of methods for minimizing electron energy spread at high first stage intensity, and calculations of second stage gain. A quasioptical cavity is proposed to contain the first-stage long-wavelength radiation while permitting transmission of second-stage short-wavelength radiation. A permanent magnet helical wiggler will be used to produce the long-wavelength radiation. At high first stage intensities ($\sim 10^8$ W/cm^2) the energy spread produced in the wiggler will be > 10% . For the experiment being proposed the beam line and electron collector must be modified to accept this spread. Companion papers in this volume give additional details of the cavity design and minimization of energy spread.

Introduction

The concept of a two-stage free electron laser was first proposed by Elias[1]. In a two-stage FEL, short-wavelength radiation is produced using a low energy electron beam. In the first stage, an electron beam with an energy on the order of a few MeV produces far infrared radiation (~ 100-1000 μm) by passing through a magnetic wiggler. This long-wavelength radiation is then backscattered from the electron beam to produce shorter-wavelength radiation (~ 1-10 μm). The long-wavelength radiation is, therefore, the pump field for the second stage of the FEL. To obtain significant gain in the second stage, a very high intensity (~ 10^7 - 10^8 W/cm^2) pump field is required.

KMS Fusion, Inc. is preparing to conduct a two-stage FEL experiment utilizing the recirculating electrostatic accelerator at The University of California Santa Barbara (UCSB)[2]. To insure the success of this experiment, all aspects of the system must be analyzed. Our studies, therefore, include investigation of the cavity design, the wiggler design, the electron beam line, the accelerator and its various components, and the FEL interaction taking place in each stage of the two-stage FEL with its appropriate scaling.

Up to this point we have concentrated on the design of the cavity and wiggler, and the scaling of each stage of the FEL. Limits on the attainable first stage power were found to be imposed by the ability of the return beam line and collector to accept the energy spread produced in the wiggler. Future studies will examine design modifications to overcome these limitations.

Resonant cavity design

To attain the high pump field intensities required to operate the second stage of the FEL, the long-wavelength radiation must be confined in a low loss resonant cavity. For example, to maintain an intracavity power of 10^8 W with 10^6 W of input power, cavity losses would have to be 10^{-2} per round trip. The input power is limited with an electrostatic accelerator by the energy the electrons could lose and still be collected in the dome of the accelerator.

For high pump field intensity both high power and a small beam diameter are needed. This high pump field intensity must be maintained over a distance of the order of meters in order to produce adequate laser gain. For the long-wavelength radiation we are considering (~ 1 mm), a long narrow beam of radiation can only be produced in a waveguide. To protect the cavity end mirrors the long wavelength beam must be permitted to expand at the ends of the cavity. It must also be possible to remove short wavelength radiation produced in the second-stage interaction without incurring significant pump field losses.

A quasioptical cavity design that could meet all of these requirements is shown in Figure 1. Long-wavelength radiation reflected from a large cavity mirror is focused down at the entrance to the waveguide. The waveguide provides a long region of uniform cross section for the FEL interaction to take place. After leaving the waveguide the long-wavelength beam expands by diffraction. The short-wavelength beam suffers almost no diffraction and passes through holes in the cavity end mirrors.

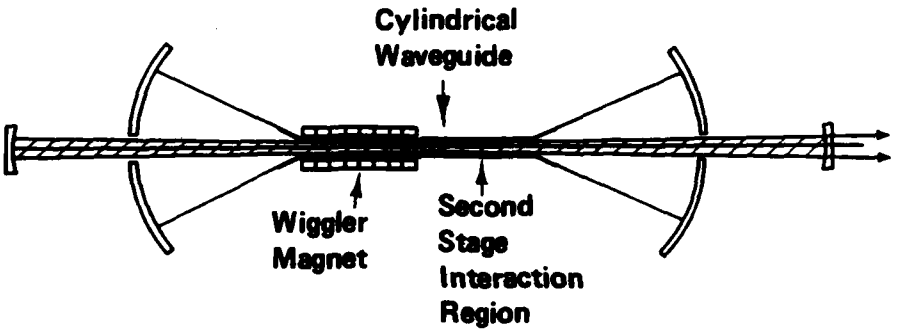

Figure 1. Conceptual design for the resonator cavity of a two-stage FEL.

The lowest loss waveguide mode in this system is the cylindrically symmetric annular TE_{01} mode. Because this mode has a minimum on axis and at the walls of the waveguide, losses are minimal at the holes in the mirror and in the waveguide. By segmenting the waveguide into conducting annular rings separated by thin insulating layers, all waveguide modes except the TE_{0N} modes could be suppressed, since these modes have wall currents with no axial component. An axial electric field could be produced in this segmented waveguide to optimize gain in both the first and second stages of the FEL.

The waveguide diameter is chosen to be much larger than the wavelength of the far infrared radiation to minimize absorption losses in the waveguide. For 1-mm radiation (300 GHz) and a waveguide inside diameter of 2.44 cm, the cutoff frequency of the guide will be 0.05 times the frequency of the long wavelength radiation. For a solid copper waveguide, the attenuation would be 1.55×10^{-4} m^{-1}. This waveguide diameter is also a convenient size for propagating a high-current (2 - 20 amp) electron beam with low wall losses.

The diameter of the electron beam must be large enough to overlap with the peak intensity region of the radiation pattern in the waveguide. An electron beam diameter of 1.6 cm is needed for the waveguide diameter that we have chosen. Space charge effects in an electron beam with an energy of a few MeV should be minimal for this beam diameter. For best overlap between the electron beam and the radiation pattern an annular beam would be preferred. However, in a filled cylindrical beam with a flat density profile most of the beam current would interact with the radiation field, so that a filled cylindrical beam would be acceptable for initial experiments.

Polarization of the TE_{01} mode is linear but varies with azimuth angle. A helical wiggler is, therefore, needed to fully excite the TE_{01} mode. The region in which second stage laser output is primarily produced is separate from the section of waveguide in which the wiggler magnet is used to produce long-wavelength radiation. This allows the gain of each stage to be optimized separately. An electron beam with low emittance and energy spread first passes through the second stage interaction region, where a very high quality beam is required to produce the short-wavelength radiation. The beam then enters the wiggler where long-wavelength radiation is preferentially produced. A small electron energy spread is produced in the second-stage interaction region, which is a negligible perturbation for the first stage FEL. A larger energy spread is produced in the first stage, because at high intensity the height of the phase space buckets is a significant fraction of the total electron energy.

The major design problem for the long-wavelength cavity is minimization of losses due to absorption, diffraction, and mode conversion. The relative importance of these losses was analyzed in an earlier report[3]. For the cavity we are considering, with copper surfaces at room temperature, absorption losses would be about half a percent per round trip pass. The only way these losses could be dramatically reduced would be by cooling the conducting surfaces in the cavity. If diffraction and mode conversion losses could be made very much smaller than absorption losses, this possibility could be considered. Diffraction losses could be made arbitrarily small by making the mirrors large enough and putting them far enough away from the waveguide so that losses around the edges and through the hole in the mirror are negligible.

Mode conversion occurs when radiation, initially in the TE_{01} mode in the waveguide, leaves the waveguide as a superposition of many free space modes, reflects off the cavity end mirror, and is refocused back into the waveguide. Because each of the free space modes suffers a slightly different phase shift along its path, the radiation pattern that is recreated at the entrance to the waveguide is not identical to the radiation pattern of the wave leaving the waveguide. Some of the radiation may, therefore, miss the entrance hole, and the radiation that re-enters the waveguide may not all be in the TE_{01} mode. Radiation not in the TE_{01} mode will suffer greater absorption losses in the waveguide and greater diffraction losses at the end mirrors.

An initial analysis of mode conversion in a quasioptical cavity composed of a cylindrical pipe and two spherical mirrors indicated that the greatest losses in the cavity would be due to mode conversion, about 1.6% per round trip pass[3] . A more detailed analysis, given in an accompanying paper[4], investigates a number of possible ways for reducing or eliminating mode conversion losses. Three techniques have been identified that could, in principle, solve this problem. One is an optical system in which the phase shift between different free space modes is exactly 2π radians or a multiple of this quantity. An optical system that does this is shown in Figure 2. In this case mode conversion losses could be eliminated[4], but absorption losses would increase due to the larger number of reflections per round trip pass. A second technique is to use a wave front matching aspheric mirror that would reflect the expanding wave exactly back on itself, eliminating phase shift between modes. A third approach is to design a microwave horn for the ends of the waveguide that would produce a transition from a single waveguide mode to a single free space mode, again eliminating the problem of relative phase shift between modes.

The wave front reflector and waveguide horn would both result in minimal absorption losses. In both cases the design is dependent on the assumed wavelength and mode pattern

produced by the wiggler. For this mode pattern losses would be extremely low, but for undesired modes the beam losses could be much higher, so that the mirror or horn would also serve as a filter for unwanted radiation.

We do not know in detail the radiation pattern that will be produced by the wiggler. The purpose of the first experiments is to determine the radiation pattern and spectrum . In this case we would prefer a cavity system that is as insensitive as possible to the wavelength, spectral distribution, and mode pattern of the emitted radiation. The design of Figure 2 is the least dependent on the radiation pattern of the possible solutions we have identified. By making the planar mirror out of a material that transmits the long-wavelength radiation, such as quartz, with a thin partially-transmitting metallic coating, it should be relatively easy to diagnose the radiation pattern that is produced. It therefore appears that the plane-parabolic mirror combination would be a good choice for initial experiments but that a wave front matching mirror or waveguide horn should be used to reduce mode conversion losses in a high-power system.

An alternative low loss cavity design has been investigated by Elias and Gallardo[5]. In this design, the long-wavelength radiation is only confined in one dimension and a linear wiggler can be used to produce the radiation field. This design does not remove the second-stage radiation through holes in the mirror, since the peak of the radiation pattern is on axis, but would require a grating or holographic plate to separate the two wavelengths in the cavity. An alternative to the single-electron beam two-stage FEL is a two-beam two-stage FEL in which a separate electron beam is used to optimize performance in each stage of the FEL. With suitable modification both the cavity design we have developed and that of Elias and Gallardo could be used in a two-electron-beam system.

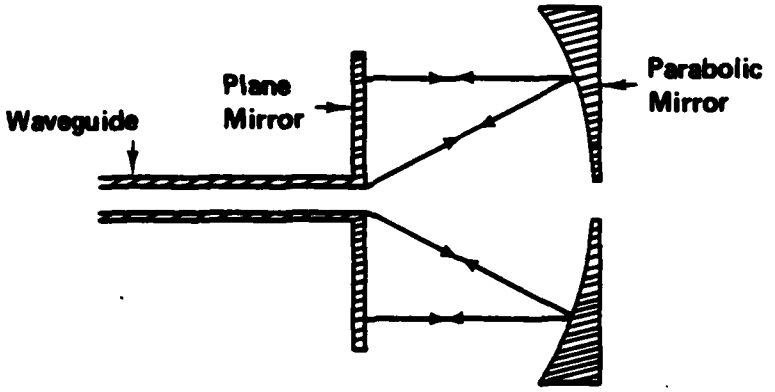

Figure 2. Multicomponent mirror system to reduce mode conversion losses.

Wiggler design

The cylindrically-symmetric quasioptical cavity design we have chosen requires a helical wiggler to fully excite the first stage TE_{01} waveguide mode. If the two-stage FEL is to develop into a practical, continuously-operating device, the wiggler magnet should not represent an energy drain. This would be the case if the wiggler were either superconducting, as is the case with the Stanford wiggler[6], or if the wiggler were made of permanent magnets.

We have decided as part of this project to develop a permanent magnet helical wiggler. This technology should be useful for many kinds of free electron lasers, not just the two-

stage FEL. No such device has yet been built, but a design for a helical wiggler based on an array of permanent magnet dipole rings has been suggested by K. Halbach[7]. To reduce this concept to a hardware design, we must develop a model to describe the field produced by an array of permanent magnets, analyze the electron orbits in the wiggler, determine conditions for beam stability, investigate injection and extraction conditions for a finite length wiggler and establish a procedure for tuning the magnets to compensate for imperfections in the magnetic material.

We have developed a three-dimensional model of the magnetic field in a helical wiggler composed of an array of permanent magnets. The field is described in the form of a Fourier series that exhibits the desired realizable helical wiggler field and its harmonics. The field has been derived for a three-dimensional cylindrical stack of segmented samarium cobalt permanent magnet dipole rings. The array is assumed to be annular and the magnetization of the segments is rotated systematically to generate a close approximation to a helical wiggler field in the innermost region.

The remanent magnetization field is represented by the double Fourier series

$$M_R = \Sigma M_{pq}(\hat{r} \cos X_{pq} + \hat{\theta} \sin X_{pq}) \tag{1}$$

where

$$X_{pq} = p\theta - qkz \ . \tag{2}$$

This becomes the source distribution used for determining the field in the inner clear-through volume, the annular region filled with magnetic material, and the region outside the annulus. The magnetic potential was found in the form of a Fourier series corresponding to the series assumed for the magnetization

$$\Psi = \Sigma T_{pq} M_{pq} \cos X_{pq} \ , \tag{3}$$

where the transfer function T(r) has a separate expression in each of the three regions. The transfer function has been found as a product of simple 2 x 2 matrices of Bessel functions and their derivatives. A similar analysis has been carried out for materials other than $SmCo_5$ with non-negligible magnetic permeability. In this analysis it was assumed that the permeability could be different in directions along and perpendicular to the easy axis. A more detailed description of the model for the magnetic field will be published separately.

To find the optimal wiggler design for this application we must determine the electron orbits in the helical wiggler and find conditions under which the beam will be stable. The electron orbits are determined by solving the equations of motion for an electron in a helical field. The problem can be simplified by choosing an appropriate coordinate system and finding constants of the motion to reduce the number of equations to be solved.

Using the exact relativistic equations for the trajectory of an electron injected into an ideal, realizable wiggler we have obtained a new constant of the motion in addition to the electron energy. To identify this constant it is convenient to choose a coordinate system that conforms to the helicity of the wiggler. For an ideal helical wiggler with no higher harmonic components of the field, the magnetic scalar potential can be written

$$\Psi = S(kr)\cos(\theta - kz)$$
$$= S(s)\cos X \tag{4}$$

where (r,θ,z) are cylindrical coordinates, $s = kr$ and $X = \theta - kz$. The coordinate system in which we choose to work is formed by three orthogonal basis vectors $\hat{r}$, $\vec{\ell}$, and $\vec{h}$. $\hat{r}$ is a unit vector in the radial direction

$$\vec{\ell} = r\nabla X \tag{5}$$

is normal to the surface of constant helicity, and

$$\vec{h} = \hat{r} \times \vec{\ell} \tag{6}$$

is tangential to the helix of constant s and X. The vectors $\vec{\ell}$ and $\vec{h}$ are not unit vectors but have the same magnitude

$$|\ell| = |h| = (1 + s^2)^{1/2} \tag{7}$$

The magnetic field is also derivable from the vector potential $\vec{A}$ which in normalized form in mks units is

$$\vec{a} = \frac{e\vec{A}}{m\gamma\beta c} \tag{8}$$

The vector potential is given by

$$k\,\hat{a} = \hat{z} \times \nabla(S(s)\sin X) \tag{9}$$

If $\hat{u}$ is a unit vector in the direction of the electron velocity, the normalized canonical angular momentum is

$$\vec{U} = \hat{u} - \vec{a}\,. \tag{10}$$

The quantity that has been found to be an exact constant of the motion is

$$V = \vec{h} \cdot \vec{U} \tag{11}$$

In cylindrical coordinates

$$V = \left(\frac{kr^2}{\beta c}\right)\frac{d\theta}{dt} + \frac{1}{\beta c}\frac{dz}{dt} - r\,\frac{dS(kr)}{dr}\sin(\theta - kz) \tag{12}$$

The significance of the conserved component of the angular momentum is that the coordinate along the helix of constant s and X plays the role of an ignorable coordinate in the equations of motion. Use of this constant allows reduction of the full equations of motion to just two second order equations for the dynamics of s and X, still subject to the constancy of the total electron energy. A full proof that V is indeed a constant of the motion will be published separately.

Computer simulations of electron orbits in an ideal helical wiggler have been performed. For injection parallel to the wiggler axis over the range of parameters that

were studied the electron orbits were always bounded, but were in general composed of oscillations at a number of different frequencies superimposed on each other (Figure 3). For nonparallel injection, conditions can be found[8] that reduce the oscillations to a single helical oscillation that would be expected to produce radiation in a well-defined narrow frequency band (Figure 4). In all cases the calculated value for V from the simulation remained constant to better than 0.5% over the length of the wiggler. We expect these studies to lead to a hardware design for a wiggler magnet that will be used together with the quasioptical cavity in an experiment utilizing the UCSB accelerator.

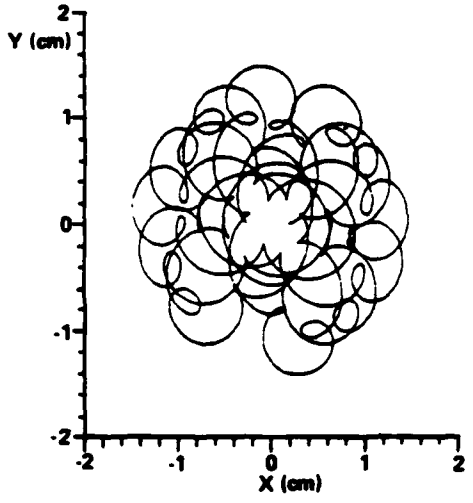

Figure 3. Bounded electron orbit for an electron injected into a helical wiggler in a direction parallel to the axis of the wiggler.

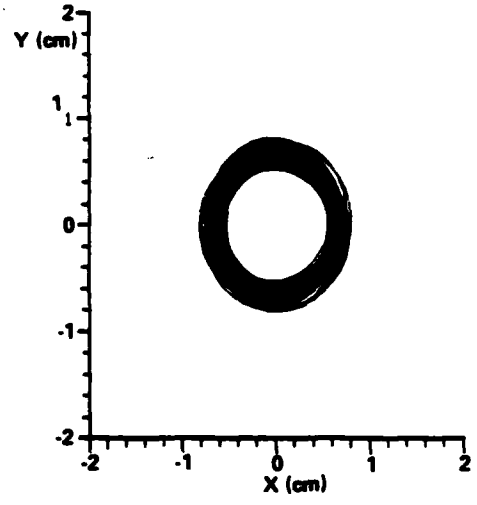

Figure 4. Orbit of an electron injected at an angle close to the pitch angle of the wiggler.

First stage amplifier design and energy spread

For the electron current that will be available from the UCSB accelerator and the anticipated second-stage cavity losses, we have determined that a very high intensity pump field ($\sim 10^7$-10^8 W/cm^2) will be required to initiate oscillations in the second stage of the two-stage FEL. Design of the first stage to attain these high intensities is, therefore, probably the most critical aspect of a two-stage FEL experiment. We have investigated a number of wiggler designs and optimization schemes that could achieve these intensities. As a result of these studies we have found limitations on the pump field intensity that could be achieved due to the inability of the return beam line and electron collector to accept an electron beam with a large energy spread in the present UCSB accelerator configuration.

The energy spread produced in the wiggler is a function of the phase space bucket height, the number of synchrotron oscillations taking place in the wiggler and the particular wiggler design. The full bucket height for zero resonant phase is given in mks units by

$$\Delta\gamma = \frac{e\lambda_w}{\pi mc}\sqrt{\frac{2}{c}}\,[E_p\,B_w]^{1/2} \qquad (13)$$

where λ_w and B_w are the wiggler period and field amplitude, respectively. E_p is the pump field amplitude, e and m are the charge and mass of the electron and c is the speed of light. The distance required for one synchrotron oscillation to take place is given by

$$L_s = \frac{\beta_z \pi}{e} \sqrt{\frac{2}{c}} \frac{\gamma mc^2}{[E_p B_w]^{1/2}} \tag{14}$$

Gain in the wiggler at high intensity must be adequate to sustain laser oscillation. Gain in the first stage must also be high enough for the pulse to grow to saturation over a small fraction of the electron pulse length in order to leave time for the second stage signal to grow from noise. The maximum gain attainable is small signal gain, G_{max}, which scales in the following way

$$G_{max} \propto B_w^2 \, J \, \lambda_w \left(\frac{L_w}{\gamma}\right)^3 \tag{15}$$

where J is the current density and L_w is the length of the wiggler.

We considered three different methods of operating the first stage:

1. Using a short, low-field constant-period wiggler that saturates at about 10^8 W/cm^2 and operates in the small signal gain regime over its entire range.
2. Using a tapered wiggler or axial electric field to trap particles and enhance gain at high intensity.
3. Using a reverse-tapered wiggler or reverse biased axial electric field to provide enhanced gain with reduced energy spread at high pump field intensities.

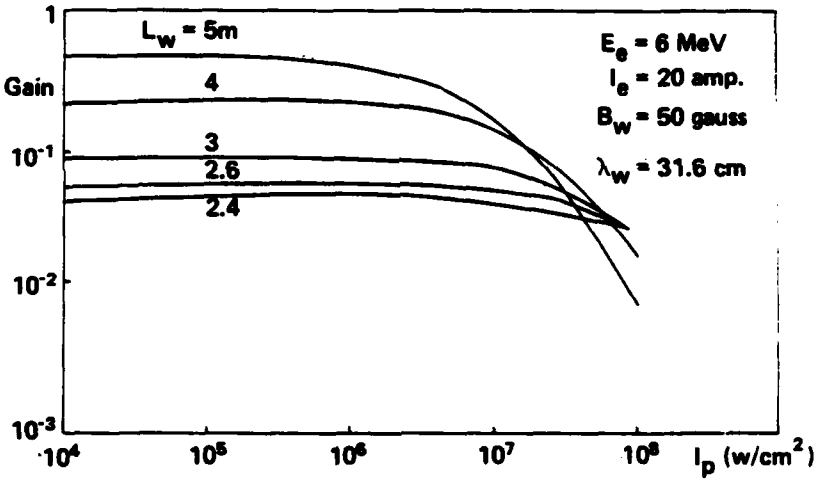

Figure 5. First stage laser gain as a function of pump field intensity for wigglers of different lengths optimized for small-signal-gain operation.

First-stage small-signal gain at constant laser wavelength was found to be greater for higher electron energies due to the longer distance required for one synchrotron oscillation and longer wiggler period. However, since for a given first-stage radiation wavelength λ_w increases approximately as γ^2, lower magnetic fields would be required to limit energy spread at higher electron beam energies. Figure 5 shows laser gain as a function of pump field intensity for a 6-MeV 20-amp electron beam producing 1-mm radiation in a wiggler with a 50-gauss magnetic field. Because the gains are calculated using a one-dimensional multiparticle simulation code assuming a filling factor of 1, actual gain in an experiment would probably be a factor of a few lower than the calculated values. Energy spread for all the cases in Figure 5 was 11.5% at 10^8 W/cm^2.

If the laser gain were only a little above threshold, a large number of passes would be required to build up to saturation intensity. Since we expect the pulse length in the UCSB accelerator to be on the order of tens of microseconds, and the gain in the second stage is expected to be low, it is desirable to operate the first stage with as high a gain as possible to minimize the fraction of the available time required for the first stage to reach saturation.

Use of a tapered wiggler to enhance laser gain at high intensity makes the energy spread problem worse than in the small signal regime. This is because a tapered wiggler only provides an advantage over an untapered wiggler when one or more synchrotron oscillations take place in the wiggler. Since the number of synchrotron oscillations increases as $B_w^{1/2}$, a significantly larger magnetic field is needed for trapping than for small signal gain optimization. The energy spread will always be larger than the bucket height in the trapping regime because untrapped electrons drift farther away from the bucket as the number of synchrotron oscillations increases (Figure 6).

The technique that appears to have the most promise for providing adequate gain and minimum energy spread at high intensity when beam recovery is required is phase space displacement. In this method, electrons move around phase space buckets which remain empty. This effect can be produced in a reverse-tapered wiggler or by applying a decelerating axial field to an electron beam traveling through a constant period wiggler. With phase space displacement the resonant phase of the bucket is negative.

Phase space displacement only produces a lower energy spread than particle trapping when there are enough synchrotron oscillations to move all electrons completely around the bucket. It is, therefore, a technique that works best with a long, high-magnetic-field wiggler and a low energy electron beam. It is possible using this method to produce an energy spread significantly smaller than the bucket height (Figure 7). A detailed discussion of phase space displacement is given in an accompanying paper[9].

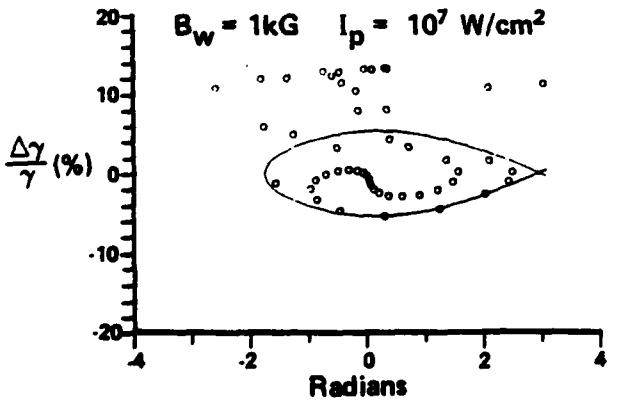

Figure 6. The energy spread produced by trapping is always greater than the bucket height at high intensities because untrapped electrons drift away from the bucket.

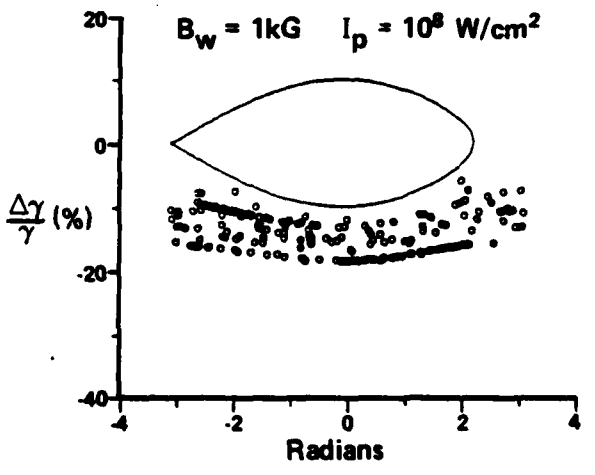

Figure 7. Phase space displacement can produce an energy spread smaller than the bucket height provided there are enough synchrotron oscillations to move all the electrons in the distribution around the buckets.

It is clear that, whatever method we use to convert electron energy to photon energy and at whatever energy we wish to operate the accelerator, a large energy spread will be produced if we try to reach a first-stage intensity of 10^8 W/cm^2. To recover the electron beam with high efficiency in the UCSB system it will therefore be necessary to redesign the beam line, so that the return line from the wiggler can accept a larger energy spread, and also to redesign the electron collector in the dome of the accelerator to accept a larger energy spread. The present accelerator and beam line are adequate, however, for single-stage low-power experiments.

Second-stage FEL scaling

Providing a number of parameters can be achieved, it should be possible to obtain on the order of 1 kw peak power in a two-stage FEL experiment using the UCSB accelerator. The parameters that are needed for a successful two-stage demonstration experiment are

$I_p \sim 10^8$ W/cm^2
$I_e \sim 20$ amp
$\tau \sim 100$ μsec

where I_p is the pump field intensity, I_e is the electron current, and τ is the length of the usable electron pulse. To operate the second-stage oscillator, laser gain must be greater than cavity losses. Second-stage gain is shown in Figure 8 for a number of different pump field intensities for an interaction length of 3 meters. Cavity losses are expected to be on the order of 1% per round trip pass in addition to the energy transmitted as output power. Because the one-dimensional simulation overestimates the gain, actual experimental gain is expected to be a factor of a few lower than calculated gain. To insure successful second stage operation we believe it will be necessary to get close to our target parameters of 10^8 W/cm^2 pump field intensity and 20 amp electron current, since small signal gain is linearly dependent on both pump field intensity and electron current. If the second stage does begin to oscillate we would expect that it would reach saturation with an intracavity intensity on the order of 10^5 W/cm^2. The cross sectional area for the interaction in the waveguide is about 1.3 cm^2 so that for 1% transmission through the output mirror a peak output power on the order of 1 kw would be achieved.

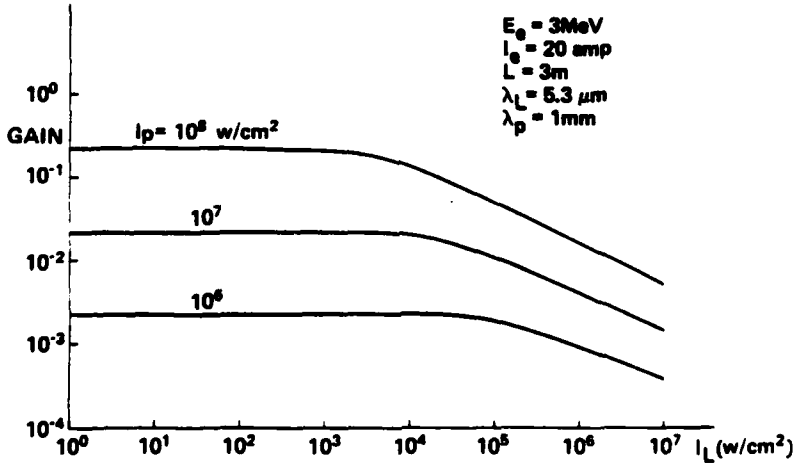

Figure 8. Second stage gain as a function of second stage laser intensity for a number of different pump field intensities and an electron current of 20 amp.

Acknowledgments

We wish to acknowledge the assistance of Alfredo Luccio of Brookhaven National Laboratory for providing us with a computer code that determines electron trajectories in a wiggler magnet. This work was supported by the U. S. Office of Naval Research.

References

1. L. R. Elias, Phys. Rev. Lett. 42, 977 (1979).
2. L. R. Elias and G. Ramian, Physics of Quantum Electronics, Volume 9, Jacobs, Pilloff, Scully, Moore, Sargent and Spitzer editors, Addison-Wesley (1982).
3. S. B. Segall, H. R. Hiddleston, H. Takeda, S. Von Laven, R. Holsinger, J. Ward, J. Richardson, and W. B. Colson, "Review of Two-Stage FEL Research at KMS Fusion", KMS Fusion Report No. KMSF-U1307, Defense Documentation Center No. AD-A128623, January (1983).
4. S. Von Laven, S. B. Segall, J. F. Ward, "A Low Loss Quasioptical Cavity for a Two-Stage Free Electron Laser", in the proceedings of this conference.
5. L. Elias and J. Gallardo, "Cylindrical Gaussian-Hermite Modes in Rectangular Waveguide Resonators" UCSB Report No. QIFEL 17/83.
6. L. R. Elias and J. M. J. Madey, Rev. Sci. Inst. 50 1335 (1979).
7. K. Halbach, Nuclear Inst. and Meth. 187, 109 (1981).
8. P. Diament, Phys. Rev. A. 23, 2537 (1981).
9. H. Takeda and S. B. Segall, "Limiting Energy Spread at High Laser Intensities using Phase Space Displacement," in the proceedings of this conference.

I. Distribution List

Director
Defense Advanced Research Projects Agency
(3 copies)
Attn: Technical Library
1400 Wilson Boulevard
Arlington, VA 22209

Office of Naval Research
(3 copies)
Physics Division Office (Code 412)
800 North Quincy Street
Arlington, VA 22217

Office of Naval Research
Director, Technology (Code 200)
800 North Quincy Street
Arlington, VA 22217

Naval Research Laboratory
(3 copies)
Department of Navy
Attn: Technical Library
Washington, DC 20375

Office of the Director of Defense Research and Engineering
(3 copies)
Information Office Library Branch
The Pentagon
Washington, DC 20301

U.S. Army Research Office
(2 copies)
Box 1211
Research Triangle Park, NC 27709

Defense Technical Information Center
(12 copies)
Cameron Station
Alexandria, VA 22314

Director, National Bureau of Standards
Attn: Technical Library
Washington, DC 20234

Commanding Officer
(3 copies)
Office of Naval Research Western Detachment Office
1030 East Green Street
Pasadena, CA 91101

Commanding Officer
(3 copies)
Office of Naval Research
Eastern/Central Detachment Off
495 Summer Street
Boston, MA 02210

Commandant of the Marine Corps
Scientific Advisor (Code RD-1)
Washington, DC 20380

Naval Ordnance Station
Technical Library
Indian Head, MD 20640

Naval Postgraduate School
Technical Library (Code 5632.2)
Point Mugu, CA 93010

Naval Ordnance Station
Technical Library
Louisville, KY 40214

Commanding Officer
Naval Ocean Research & Development Activity
Technical Library
NSTL Station, MS 39529

Naval Explosive Ordnance Disposal Facility
Technical Library
Indian Head, MD 20640

Naval Ocean Systems Center
Technical Library
San Diego, CA 92152

Naval Surface Weapons Center
Technical Library
Silver Springs, MD 20910

Naval Ship Research & Development Center
Central Library (Code L42 and L43)
Bethesda, MD 20084

Naval Avionics Facility
Technical Library
Indianapolis, IN 46218

DD FORM 1 JAN 73 1473 EDITION OF 1 NOV 65 IS OBSOLETE

SECURITY CLASSIFICATION OF THIS PAGE (When Data Entered)